

EXPERIMENTAL SIGNALS OF THE FIRST PHASE TRANSITION OF NUCLEAR MATTER

B. BORDERIE

Institut de Physique Nucléaire, IN2P3-CNRS, F-91406 Orsay Cedex, France.

Vaporized and multifragmenting sources produced in heavy ion collisions at intermediate energies are good candidates to investigate the phase diagram of nuclear matter. The properties of highly excited nuclear sources which undergo a simultaneous disassembly into particles are found to sign the presence of a gas phase. For heavy nuclear sources produced in the Fermi energy domain, which undergo a simultaneous disassembly into particles and fragments, a fossil signal (fragment size correlations) reveals the origin of multifragmentation: spinodal instabilities which develop in the unstable coexistence region of the phase diagram of nuclear matter. Studies of fluctuations give a direct signature of a first order phase transition through measurements of a negative microcanonical heat capacity.

1 Introduction

The decay of highly excited nuclear systems through a simultaneous disassembly into fragments and particles, what we call multifragmentation, is a subject of great interest in nuclear physics. Indeed multifragmentation should be related to subcritical and/or critical phenomena. Thus it is fully connected to the nature of the phase transition which is expected of the liquid-gas type due to the specific form of the nucleon-nucleon interaction; as van der Waals forces, the nucleon-nucleon interaction is characterized by attraction at long and intermediate range and repulsion at short range.

Although multifragmentation has been observed for many years, its experimental knowledge was strongly improved only recently with the advent of powerful devices built in the last decade. Selecting the “simplest” experimental situations, well defined systems or subsystems which undergo vaporization (simultaneous disassembly into particles) or multifragmentation can be thus identified and studied.

It is a difficult task to deduce information on the phase diagram and the related equation of state of nuclear matter from nucleus-nucleus collisions at intermediate energies. But it is also a very exciting novel physics in relation with thermodynamics of finite systems (connection to other fields) without external constraints (pressure, volume) ^{1,2}.

2 From multifragmentation to vaporization : identification of the gas phase

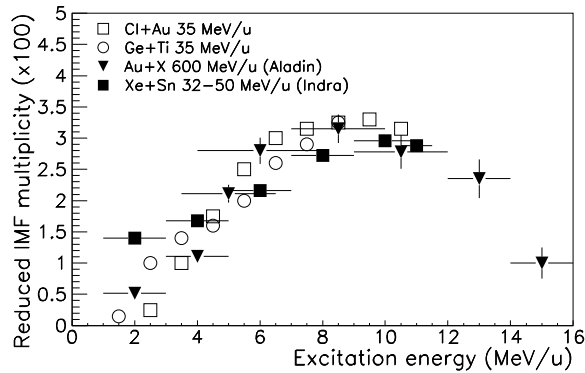


Figure 1. Fragment multiplicity (normalised to the number of incident nucleons) as a function of the excitation energy. (from ³).

Let us first locate in which excitation energy domain multifragmentation takes place. Fig 1 indicates the evolution of the reduced (normalised to the size of the multifragmenting system) fragment multiplicity as a function of the excitation energy per nucleon of the system. A universal behavior characterized by a bell shape curve is observed. The onset of multifragmentation is observed for excitation energies around 3 MeV per nucleon, the maximum for fragment production is found around 9 MeV per nucleon, i.e. close to the binding energy of nuclei. At higher excitation energy, the opening of the vaporization channel reduces fragment production.

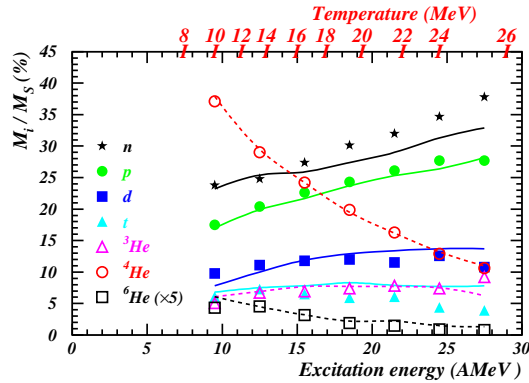


Figure 2. Composition of vaporized quasi-projectiles, formed in 95 A MeV $^{36}\text{Ar}+^{58}\text{Ni}$ collisions, as a function of their excitation energy per nucleon. Symbols are for data while the lines (dashed for He isotopes) are the results of the model. The temperature values used in the model are also given. (from ⁴).

The gas phase has been identified by studying the deexcitation properties

of vaporized quasi-projectiles with A around 36⁴. Chemical composition (first and second moments) and average kinetic energies of the different particles are well described by a gas of fermions and bosons in thermal and chemical equilibrium. Inclusion of a van der Waals-like behavior (final state excluded volume) was found decisive to obtain the observed agreement (see for example figure 2). In the model, the experimental range in excitation energy per nucleon of the source was covered by varying the temperature from 10 to 25 MeV and the free volume was fixed at $3V_0$, which corresponds to an average inter-distance between particles of about 2 fm, close to the range of the nuclear force (freeze-out configuration).

3 Thermometry and calorimetry : caloric curves and first-order phase transition ?

The plateau observed in the shape of the caloric curve (determined from calorimetry and nuclear thermometry) was proposed by the ALADIN collaboration a few years ago as a signature of a first-order phase transition⁵. Since this observation works from different collaborations, covering a large range in mass of nuclei, have been published^{6,7,8,9}. Many caloric curves have been obtained which can roughly be classified in two groups depending on the nuclear thermometer chosen (isotopic double ratios using $({}^6\text{Li}/{}^7\text{Li})/({}^3\text{He}/{}^4\text{He})$ or $(\text{d}/\text{t})/({}^3\text{He}/{}^4\text{He})$). Moreover the presence of a plateau was not confirmed in these studies, even by the ALADIN collaboration when looking at properties of target-like spectators in Au+Au collisions at 1000AMeV¹⁰. All these studies clearly indicate that no decisive signal can be extracted. We do not have an absolute nuclear thermometer and above all, experimentally one does not explore the caloric curve at constant pressure nor at constant volume. In fact measured caloric curves are sampling a monodimensional curve on the microcanonical equation of state surface (T versus energy and volume)^{2,11}; for each energy of the system a different average volume at freeze-out (no more nuclear interaction) is obtained, depending on the observed partition.

4 Statistical and dynamical descriptions of multifragmentation

Many theories have been developed to explain multifragmentation (see for example ref.¹² for a general review of models). Among the models some are related to statistical approaches^{13,14}, valid at and after freeze-out, whereas others try to describe the dynamical evolution of systems, from the beginning of the collision between two nuclei to the fragment formation^{15,16}. I shall very briefly focus here on two models which will be compared later on to ex-

perimental data. Firstly a statistical description of multifragmentation (SMM model ¹⁴), in which an equilibration of a system at low density is assumed. Then the statistical weight of a given break-up channel f , i.e. the number of microscopic states leading to this partition, is determined by its entropy $\Delta\Gamma_f = \exp S_f$ within the microcanonical framework. In such an approach the initial parameters as the mass and charge of the multifragmenting system, its excitation energy, its volume (or density) and the eventual added radial expansion have to be backtraced to experimental data. Secondly, dynamical stochastic mean-field simulations which are obtained by restoring fluctuations in deterministic one-body kinetic simulations. In particular in such simulations, relative to the standard nuclear Boltzmann treatment, an approximate tool is provided by introducing a noise by means of a brownian force in the mean field (Brownian One-Body (BOB) dynamics ^{17,18}). The magnitude of the force is adjusted to produce the same growth rate of fluctuations as the full Boltzmann-Langevin theory ¹⁹. Such simulations completely describe the time evolution of the collision and thus help in learning about nuclear matter and its phase diagram whereas statistical models start from the phase diagram and have more to do with the thermodynamical description of finite nuclear systems.

Both descriptions have been successful in reproducing average static and kinematical properties of fragments (see for example ref. ²⁰). They will be compared in what follows to more constrained observables which are expected to bring decisive information on the origin and properties of multifragmentation.

5 Correlations in events: spinodal instabilities and equilibration

5.1 Fragment size correlations: a fossil signature

Dynamical simulations predict that during a central collision between heavy nuclei in the Fermi energy domain (30-40 MeV per nucleon incident energies) a wide zone of the phase diagram is explored (gentle compression-expansion cycle) and the fused system enters the liquid-gas coexistence region (at low density) and even more precisely the unstable spinodal region (domain of negative incompressibility). Thus a possible origin of multifragmentation may be found through the growth of density fluctuations in this unstable region. Within this theoretical scenario a breakup into nearly equal-sized “primitive” fragments should be favored in relation with the wave-lengths of the most unstable modes present in the spinodal region ²¹. However this picture is

expected to be blurred by several effects: the beating of different modes, the presence of large wave-length instabilities and eventual coalescence of nascent fragments. Then how to search for a possible “fossil” signature of spinodal decomposition? A few years ago a new method called higher order charge correlations was proposed in ²². All fragments in one event (average fragment charge $\langle Z \rangle$ and the standard deviation per event ΔZ) are used to build the charge correlation for each fragment multiplicity.

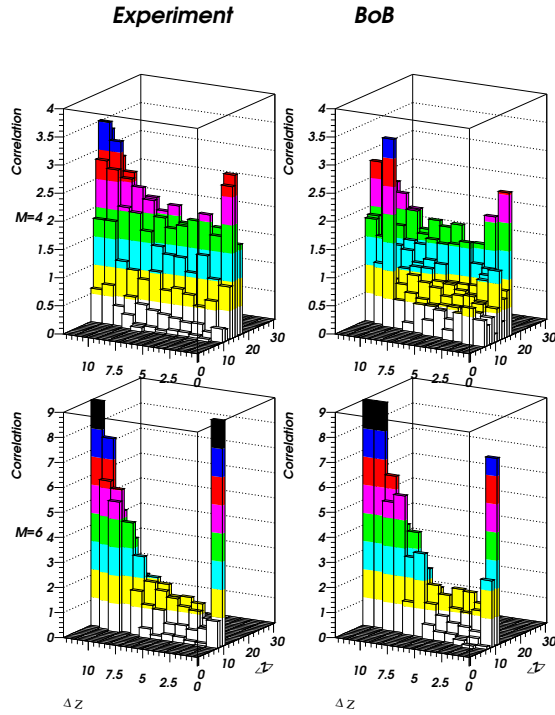


Figure 3. Fragment charge correlations from fused events produced in central collisions between Xe and Sn at 32 MeV per nucleon incident energy: comparison between experiment (left) and BOB calculations (right) for fragment multiplicities equal to 4 and 6. (from ²⁰).

Figure 3 shows results from ²⁰ for such correlation functions in experimental fusion events and BOB simulated events (Xe+Sn system at 32 MeV per nucleon). For all fragment multiplicities the charge correlation has a peak in the bin $\Delta Z = 0-1$, indicating an enhancement of partitions with equal-sized fragments. This weak but non ambiguous enhancement (0.1% of events if we restrict to the bin 0-1 and about 1% if we enlarge to bin 1-2 to take into account secondary decays of fragments) is interpreted as a signature of spinodal instabilities as the origin of multifragmentation in the Fermi energy

domain. Moreover the occurrence of spinodal decomposition signs the presence of a liquid-gas coexistence region and consequently, although indirectly, a first order phase transition.

5.2 *Fragment-particle correlations: equilibrium at freeze-out*

Fragment-particle velocity correlations in events have been proposed to experimentally measure excitation energy of hot primary fragments produced in multifragmentation²³. By means of this technique multiplicities and relative kinetic energy distributions between fragments and light charged particles that they evaporate are determined to reconstruct the excitation energies of fragments. For the Xe+Sn reaction, the INDRA collaboration has measured the evolution of the average excitation energy per nucleon of primary fragments produced in multifragmentation of fused systems at different incident energies (from 32 to 50 MeV per nucleon)²⁴. Within the error bars a constant value around 3.0-3.5 MeV per nucleon was measured in good agreement with the approach at equilibrium (SMM). This suggests that equilibrium is reached at freeze-out. Note that dynamical simulations (BOB) performed at 32 MeV per nucleon also predict the same excitation of fragments at freeze-out²⁰.

How to reconcile the dynamical (spinodal instabilities) and statistical (equilibrium at freeze-out) aspects which have been extracted from correlations ? The following scenario can be proposed: spinodal instabilities cause multifragmentation but when the system reaches the freeze-out stage, it has explored enough of the phase space in order to be describable through an equilibrium approach.

6 Kinetic energy fluctuations and negative microcanonical heat capacity

Within the microcanonical equilibrium framework, it was recently shown^{25,2} that for a given total energy of a system, the average partial energy stored in a part of the system is a good microcanonical thermometer, while the associated fluctuations can be used to construct the heat capacity (see²). In presence of a phase transition large fluctuations are expected to appear as a consequence of the divergence and of the possible negative branch of the microcanonical heat capacity. From experiments the most simple decomposition of the total energy E^* is in a kinetic part E_1 and a potential part E_2 (Coulomb energy + total mass excess). However these quantities have to be determined at freeze-out and consequently it is necessary to trace back this configuration on an event by event basis. The true configuration needs the knowledge of all the charged

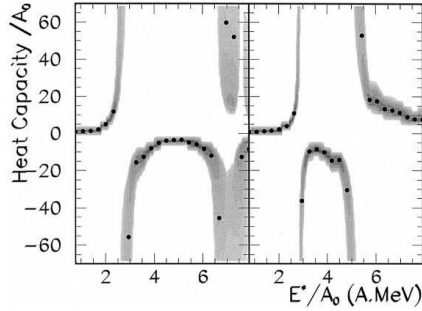


Figure 4. Measurements of microcanonical heat capacity per nucleon (symbols) as a function of the excitation energy per nucleon for quasi-projectiles produced in Au+Au collisions. The two panels refer to different freeze-out hypotheses. The grey contour indicates the confidence region for C_t . (from ²⁶).

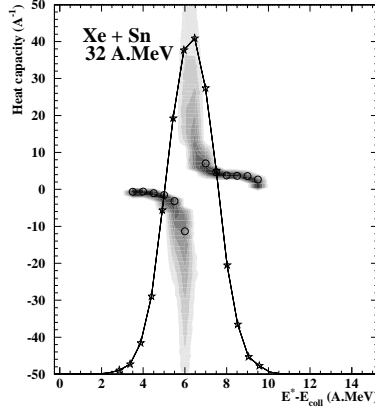


Figure 5. Same as figure 4 for fused nuclei produced in central collisions between Xe and Sn at 32 MeV per nucleon incident energy. (from ²⁷).

particles evaporated from primary hot fragments and of the undetected neutrons; consequently some reasonable hypotheses have to be done. Note also that fragment-particle correlations discussed just before can help to obtain a better knowledge of freeze-out configurations (see ²⁸). Then the experimental correlation between the kinetic energy per nucleon E_1/A_0 and the total excitation energy per nucleon E^*/A_0 of the considered system can be obtained as well as the reduced variance of the kinetic energy $\sigma_1^2 / \langle E_1^2 \rangle$. Finally the microcanonical temperature of the system can be obtained by inverting the kinetic equation of state and the total microcanonical heat capacity C_t is extracted from the following equations:

$$C_1 = \frac{\delta \langle E_1/A_0 \rangle}{\delta T} \quad \text{and} \quad C_t = \frac{C_1^2}{C_1 - \frac{A_0 \sigma_1^2}{T^2}}$$

Figures 4 and 5 show results obtained by M. D'Agostino et al. and the INDRA collaboration for hot nuclei with mass number around 200 formed in different experimental conditions. In figure 4 the microcanonical heat capacity is calculated over a large excitation energy range for quasi-projectiles (formed in Au+Au collisions at 35 MeV per nucleon incident energy) assuming two different hypotheses to trace back freeze-out configurations; figure 5 refers to

fusion events produced in central Xe+Sn collisions at 32 MeV per nucleon; in this latter case, a narrower excitation energy distribution (bell shape curve on the figure) is observed. A distinct negative branch is observed, revealing a first order phase transition. The distances between the poles are associated with the latent heat. Note that the same location of the pole at high excitation energy is found when similar hypotheses are made for freeze-out reconstruction (left part of figure 4 and figure 5).

7 Signatures of critical behavior

For finite systems, related to the correlation length, a critical region instead of a critical point is expected. The following signatures of critical behavior were reported: power laws have been observed within selected conditions, critical exponents have been measured in agreement with those of a liquid-gas model^{29,26} assuming that fragment multiplicity or thermal excitation energy is the control (“order”) parameter and a nuclear scaling function has been evidenced by the EOS collaboration²⁹. However, as compared to infinite systems, potential divergences are smoothed over finite regions of the chosen control parameter and the choice of the fit regions where the data are assumed to reflect the critical behavior is crucial. Clearly one needs a precise and objective procedure in order to determine order parameters and critical signals. Such a methodology was recently proposed for second order phase transitions³⁰ and we can expect in the future to dispose of a similar methodology for first order phase transitions.

8 Conclusions

A set of coherent results showing the existence of a first order phase transition in nuclear matter has been obtained and the two signals observed related to correlations and fluctuations constitute a strong starting point for systematic investigations. Clearly caloric curves do not and can not give a decisive signal of a first order phase transition. Selected data have properties compatible with the equilibrium hypothesis at freeze-out and this framework is up to now chosen for progressing in the experiment-theory interaction. Experimentally an effort has to be made to better define configurations at freeze-out, which are key points to bring more quantitative information (latent heat...). On the theoretical side, concerning thermodynamics of finite systems, some improvements are needed in lattice gas models for example to take into account the specificities of nuclei (quantal aspects and Coulomb interaction). Concerning the signatures of critical behavior and the definition of the critical

region, experimentalists need a methodology dedicated to first order phase transition for finite systems.

I am highly indebted to my colleagues of the INDRA collaboration and to R. Botet, X. Campi, Ph. Chomaz, M. Colonna, M. D'Agostino and F. Gulminelli for valuable discussions.

References

1. D.H. E. Gross, this conf.
2. Ph. Chomaz, this conf.
3. D. Durand, *Nucl. Phys. A* **630**, 52c (1997).
4. B. Borderie *et al.*, (INDRA coll.), *Eur. Phys. J. A* **6**, 197 (1999).
5. J. Pochodzalla *et al.*, (ALADIN coll.) *Phys. Rev. Lett.* **75**, 1040 (1995).
6. Y. G. Ma *et al.*, (INDRA coll.) *Phys. Lett. B* **390**, 41 (1997).
7. J. A. Hauger *et al.*, (EOS coll.) *Phys. Rev. C* **57**, 764 (1998).
8. K. Kwiatkowski *et al.*, *Phys. Lett. B* **423**, 21 (1998).
9. J. Cibor *et al.*, *Phys. Lett. B* **473**, 29 (2000).
10. W. Trautmann for the ALADIN coll., *Advances in Nuclear Dynamics 4* (1998) p.349.
11. Ph. Chomaz, V. Duflot and F. Gulminelli Ganil report P 00 01.
12. L. G. Moretto and G. J. Wozniak, *Ann. Rev. of Nuclear and Particle Science* **43**, 379 (1993) and references therein.
13. D.H.E. Gross, *Rep. Prog. Phys.* **53**, 605 (1990) and references therein.
14. J. Bondorf *et al.*, *Phys. Rep.* **257**, 133 (1995) and references therein.
15. A. Guarnera *et al.*, *Phys. Lett. B* **373**, 267 (1996).
16. A. Ono and H. Horiuchi, *Phys. Rev. C* **53**, 2958 (1996).
17. Ph. Chomaz *et al.*, *Phys. Rev. Lett.* **73**, 3512 (1994).
18. A. Guarnera *et al.*, *Phys. Lett. B* **403**, 191 (1997).
19. Ph. Chomaz, *Ann. Phys. Fr.* **21**, 669 (1996).
20. M. F. Rivet *et al.*, (INDRA coll.) this conf. and references therein.
21. S. Ayik *et al.*, *Phys. Lett. B* **353**, 417 (1995).
22. L. G. Moretto *et al.*, *Phys. Rev. Lett.* **77**, 2634 (1996).
23. N. Marie *et al.*, *Phys. Rev. C* **58**, 256 (1998).
24. S. Hudan *et al.*, (INDRA coll.) Proc. Bormio (2000), p. 443.
25. Ph. Chomaz and F. Gulminelli, *Nucl. Phys. A* **647**, 153 (1999).
26. M. D'Agostino *et al.*, *Phys. Lett. B* **473**, 219 (2000).
27. N. Le Neindre *et al.*, (INDRA coll.) this conf.
28. M. D'Agostino *et al.*, this conf.
29. J.B. Elliot *et al.*, (EOS coll.) *Phys. Lett. B* **418**, 34 (1998).
30. R. Botet and M. Ploszajczak, Ganil report P 00 17.